Integration Design of Passive Filtering Nonmagnetic Circulator Based on Spatiotemporal Modulation of Microstrip Filtering Delay Networks

Daotong Li, *Senior Member, IEEE*, Chen Yang, Ying Liu, Luqi Zhang, and Qiang Chen, *Senior Member, IEEE*

***Abstract*— A novel filtering nonmagnetic circulator based on the spatiotemporal modulation of microstrip filtering delay network using traditional PCB processing technology is presented in this article. By utilizing switches controlled by periodic signal to realize spatiotemporal modulation of microstrip filtering delay networks with large and flat in-band group delay response, the symmetry of time reversal is broken and thus the nonreciprocity characteristic is realized. By combining the advantages of both circulators and filters, a filtering nonmagnetic circulator is thus constructed. It is worth noting that all the circuit elements are fabricated using the traditional PCB technology, which is easy to integrate with other systems. The working mechanism is investigated theoretically and numerically. Moreover, the transmission characteristics and the group delay of the microstrip filtering delay network, which play a key role in spatiotemporal modulation in the proposed nonmagnetic circulator, are analyzed in detail. The prototype of the proposed filtering nonmagnetic circulator is designed, simulated, fabricated, and measured. The measured results agree well with the simulated ones. The nonmagnetic filtering circulator operates at 930–990 MHz with a relative bandwidth of 6.25%, and good filtering characteristics are also obtained. The maximum isolation of the circulator in the passband is better than −20 dB and the insertion loss (IL) is only 2.6 dB. Due to the compact microstrip filtering delay network with large group delay is used to realize the filtering and delay function in the system, good filtering characteristics are integrated into the nonmagnetic circulator, and the oversize is also reduced.**

Manuscript received 27 March 2023; revised 22 June 2023 and 22 July 2023; accepted 24 July 2023. Date of publication 15 September 2023; date of current version 7 February 2024. This work was supported in part by the National Natural Science Foundation of China under Grant 61801059, in part by the FY2021 Japan Society for the Promotion of Science (JSPS) Postdoctoral Fellowship for Research in Japan under Grant P21053, in part by the Grant-in-Aid for JSPS Research Fellow under Grant 21F21053, in part by the Opening Fund of State Key Laboratory of Millimeter Waves under Grant K202016, and in part by the Basic Research and Frontier Exploration Special of Chongqing Natural Science Foundation under Grant cstc2019jcyj-msxmX0350. *(Corresponding author: Daotong Li.)*

Daotong Li is with the Center of Aerocraft TT&C and Communication, Chongqing University, Chongqing 400044, China, also with the School of Microelectronics and Communication Engineering, Chongqing University, Chongqing 400044, China, and also with the Department of Communications Engineering, Tohoku University, Sendai 980-8579, Japan (e-mail: dli@cqu.edu.cn).

Chen Yang, Ying Liu, and Luqi Zhang are with the School of Microelectronics and Communication Engineering, Chongqing University, Chongqing 400044, China.

Qiang Chen is with the Department of Communications Engineering, Tohoku University, Sendai 980-8579, Japan.

Color versions of one or more figures in this article are available at https://doi.org/10.1109/TMTT.2023.3311918.

Digital Object Identifier 10.1109/TMTT.2023.3311918

***Index Terms*— Circulator, filtering, flat group delay, nonmagnetic, nonreciprocity.**

I. Introduction

THE co-time co-frequency full duplex system, as shown in Fig. 1, has become more and more important in today's rapidly developing communication systems, and the co-frequency self-interference suppression characteristics is urgently required in the full duplex system [1], [2], [3]. The self-interference cancellation has mainly three methods: antenna-based [4], nonreciprocal system [5], and mixed-signal [6]. The antenna-based method requires at least two antennas to achieve self-interference cancellation by applying an inverse signal to the receiving terminals that is exactly opposite to its transmitted signal, but this depends on the antenna locations and the extremely high antenna performance requirements. The mixed-signal approach uses a feed-forward, passive, wideband, cancellation scheme to subtract the transmitter signal at the receiver node. This method is more complex to design and is prone to cause additional interference. The circulator, which is one of the methods to realize self-interference cancellation, has also received more attention from researchers [7], [8].

Conventional circulators are based on the ferrite materials, the magnetic moment within the material is given a preferred direction of rotation under the condition of external magnetic field bias to break the nonreciprocity. However, traditional ferrite circulators are bulky and incompatible with conventional silicon-based integration processes [9], [10]. Recently, the realization of the nonreciprocity properties of the system under nonmagnetic conditions has attracted the attention of researchers. A nonmagnetic nonreciprocity metamaterial based on a ring resonator loop loaded by an active transistor has been proposed [11], [12], where the transistor is biased by the dc voltage to produce a rotating magnetic moment similar to that in ferrites, causing the electromagnetic wave in the ring to travel in only one direction. However, the noise and nonlinear distortion of the system will increase due to active-biased transistors. Spatiotemporal modulation of waveguides based on electrical or acoustic signals to achieve nonreciprocity is reported in [13], [14], and [15]. Due to the weakness of electro-optic and acousto-optic effects, it requires bulky equipment and relies on nonuniform modulation across the

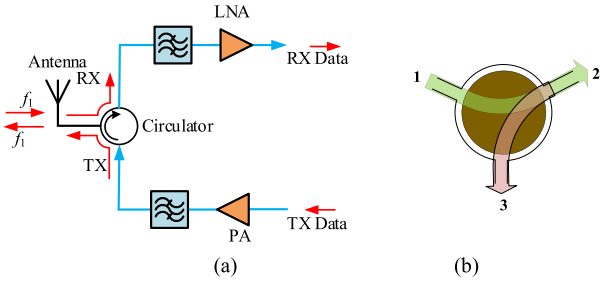

Fig. 1. (a) Co-time co-frequency full-duplex system. (b) Three-port circulator.

waveguide cross section, which increases the complexity of the manufacturing process. Some literatures reported nonmagnetic circulators by employing the spatiotemporal modulation of the ring resonator with a phase difference of 120°, but its operating frequency band is narrow, and the IL is large due to the spectral leakage of the modulation port [16], [17], [18], [19]. The nonmagnetic circulator is first implemented using filters and switches in [20], and since six AlN MSMS filters and an asymmetric structure are employed, its size, insertion loss (IL), and system complexity should be improved. In addition, the authors proposed a modeling method to model a switch as a resistor in parallel with a current-controlled current source (CCCS) to achieve a good accuracy of circulator analysis in [21]. Recently, some scholars put forward the design theory of network based on switches and delay lines, but the delay lines are often bulky and do not have frequency selectivity characteristics. In practice, external filters are usually required to realize frequency selectivity, which is not conducive to system integration. In response, the replacement of the delay line module with the surface acoustic wave (SAW) filters has been proposed by some scholars, but the SAW structures are also not conducive to system integration because of the difference in processing technologies [22], [23], [24], [25], [26], [27].

In this article, a filtering nonmagnetic circulator based on the spatiotemporal modulation of a microstrip filtering delay network using traditional PCB processing technology is presented. Benefiting from the filtering characteristics and flat in-band group delay of the proposed microstrip filtering delay network, the circulator combines the advantages of both the microstrip filtering structure and nonreciprocal network simultaneously. Moreover, the integrated design of the delay module and microstrip filtering structure realizes the miniaturization and multifunctional integration of the nonmagnetic filtering circulator. First, the theoretical basis related to the proposed filtering nonmagnetic circulator is presented. Then, the impacts of filtering response, group delay, and time modulations on the proposed nonmagnetic filtering circulator are analyzed theoretically and numerically. Furthermore, the microstrip filtering delay network with good selectivity and large group delay characteristics is designed, analyzed, fabricated, and measured. Finally, for demonstration, a filtering nonmagnetic circulator with the center frequency of 960 MHz, fractional bandwidth (FBW) of 6.25%, in-band isolation of −20 dB, and good filtering performance based on the spatiotemporal modulation of the microstrip filtering delay network is designed, fabricated, assembled, and measured, which verifies the effectiveness of the design methodology.

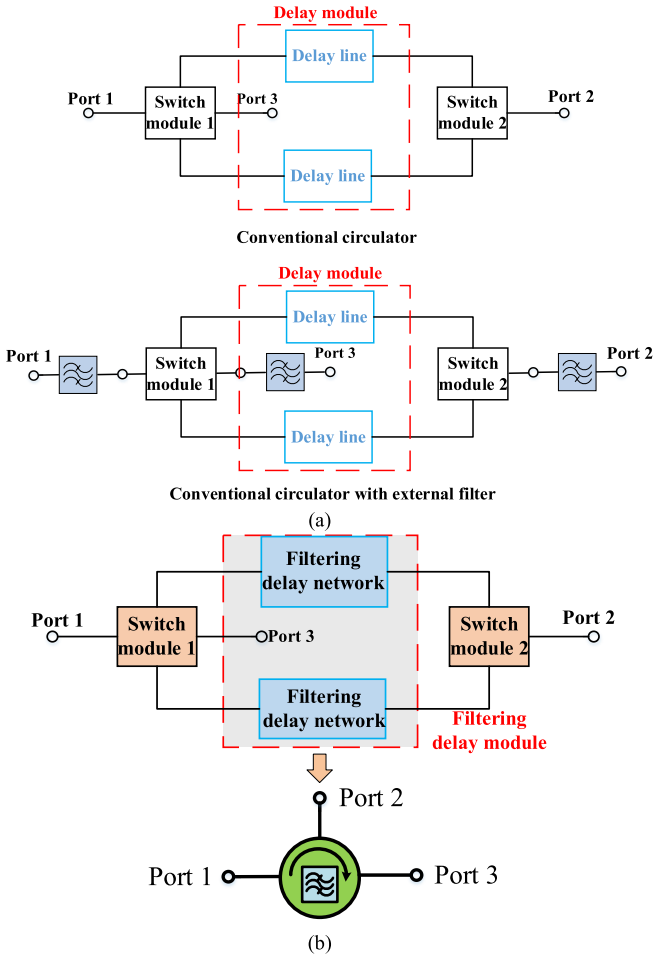

Fig. 2. Schematic of (a) conventional circulator and (b) proposed filtering nonmagnetic circulator.

II. Theoretical Analysis

Generally, a circulator is a passive, nonreciprocal three- or four-port device that only allows a microwave or radio frequency signal to exit through the port immediately following the port it entered. For a three-port circulator, a signal applied to port 1 will only come out of port 2, a signal applied to port 2 only come out of port 3, a signal applied to port 3 only come out of port 1, and so on, as shown in Fig. 1(b).

A. Theoretical Analysis of Filtering Nonmagnetic Circulator

The circulators usually consist of switch modules and delay line modules, as shown in Fig. 2. The delay lines used to provide group delay characteristics usually have a relatively large size and IL, which makes the whole circulator larger in size and deteriorates the transmission performance. Meanwhile, since the circulator has no filtering function, external filters are usually required to suppress the out-of-band interference in practical applications, which makes the whole system become redundant and not easy to integrate. Herein, the filtering nonmagnetic circulator is proposed by integrating the microstrip filtering structure and delay line together, which incorporates the microstrip filtering structure into the delay line modules. Moreover, the proposed microstrip

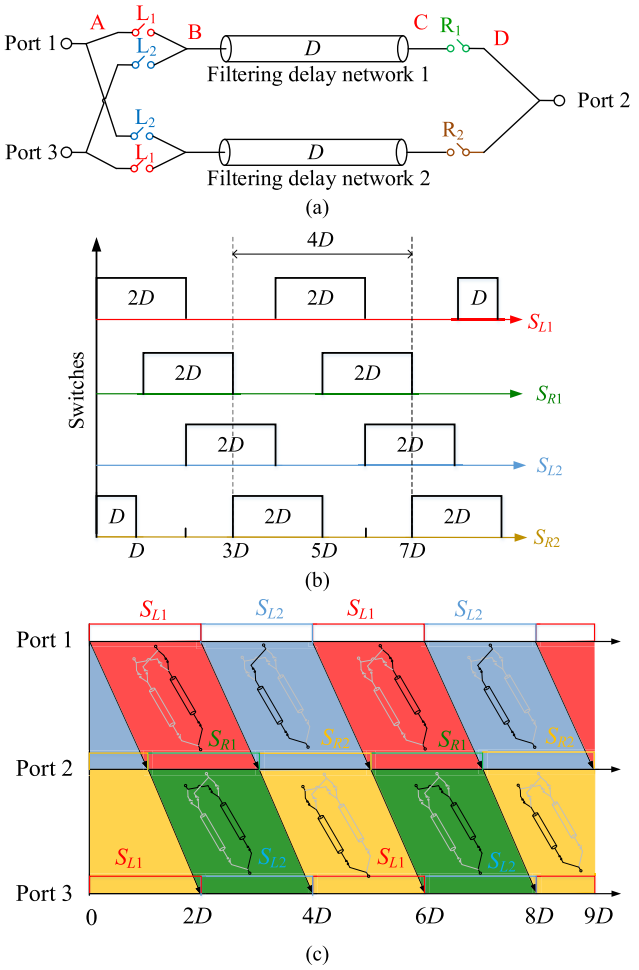

Fig. 3. Proposed passive nonmagnetic filtering circulator. (a) Schematic of the proposed three-port circulator. (b) Controlling signal of switches. (c) Operating principle of the circulator.

filtering delay network has the advantages of filtering response, smaller size, and lower IL compared with the traditional delay line, and thus, the miniaturization and lightweight of the system are further realized.

B. Operating Principle of Nonmagnetic Circulator

As shown in Fig. 3(a), the proposed filtering nonmagnetic circulator consists of three single pole single throw (SPSD) switches and two filtering delay networks, and the switches are controlled by the periodic signals shown in Fig. 3(b). Through the periodic "ON" and "OFF" of the switches and the filtering delay networks, the functions of the proposed filtering circulator are realized. The period of the controlling signal is four times the group delay of the filtering network's ($4D$) is used to control the switches, and the phase differences of D are assigned between the four periodic signals, which are expressed as follows:

$$S_{L1}(t) = \sum G_{2D}(t/4D - 0.25 - N) \tag{1}$$

$$S_{R1}(t) = \sum G_{2D}(t/4D - 0.5 - N) \tag{2}$$

$$S_{L2}(t) = \sum G_{2D}(t/4D - 0.75 - N) \tag{3}$$

$$S_{R2}(t) = \sum G_{2D}(t/4D - 1 - N) \tag{4}$$

where $G_{2D}(t)$ is the window function signal, and N is the number of periods of the signal. When the signal of the control switch is 1, the switch is in the "ON" state; that is, the switch is completely short-circuited, and when the signal is 0, the switch is in the "OFF" state, which means that the switch is completely disconnected. Thus, the periodic "ON" and "OFF" of the three groups of switches can be realized.

The working principle of the proposed filtering nonmagnetic circulator is shown in Fig. 3(c), assuming that there is no delay in the "ON" and "OFF" states of the switches. At time $t = 0$, the signal is fed to port 1, it can be known that S_{L1} and S_{R2} are at the "ON" states, and the signal of port 1 is further fed to the filtering delay network 1 through S_{L1}. And after the delay time D, S_{R1} is turned "on," and the signal can enter port 2 through S_{R1} to realize the transmission from port 1 to port 2. At time $t = D$, the signal from port 2 enters the filtering delay network through S_{R1}. After another delay time D, S_{L1} is turned "on," and S_{L2} is turned "off," so the signal from port 2 cannot be transmitted to port 1, but enters port 3, the time-reversal symmetry is thus broken, and the nonreciprocal function of the circulator is realized.

C. Frequency-Domain Analysis

In order to further investigate the working mechanism of the proposed filtering nonmagnetic circulator, the frequency-domain analysis is carried out. Assuming that only port 1 has an input signal, the excitation signal $S_A(t)$ enters from port 1, and $S_B(t)$, $S_C(t)$, and $S_D(t)$ are successively generated by the excitation signal after passing through the switch L_1, the filtering delay network and the switch R_1, where the control signal in the frequency domain can be expressed as follows:

$$S_{L1}(\omega) = \frac{1}{2}\delta(\omega) + \sum_{n=1}^{\infty}\left\{\frac{j}{n\pi}\sin\left(\frac{n\pi}{2}\right)[\delta(\omega+n\omega_m) - \delta(\omega - n\omega_m)]\right\} \tag{5}$$

where ω_m is the switching modulation signal angular frequency, $\delta(\omega)$ is the impulse function, and ω is the frequency. The signal $S_B(t)$, $S_C(t)$, and $S_D(t)$ can be expressed in the frequency domain as follows:

$$S_B(\omega) = S_A(\omega) * S_{L1}(\omega) \tag{6}$$

$$S_C(\omega) = S_B(\omega) * F_{GD}(\omega) = S_B(\omega) \cdot e^{-j\omega D} \tag{7}$$

$$S_D(\omega) = S_C(\omega) * S_{R1}(\omega) = \left[S_B(\omega) \cdot e^{-j\omega D}\right] * S_{R1}(\omega) \tag{8}$$

where $F_{GD}(\omega)$ is the transfer function of the filtering delay network module. The time-harmonic components in (6) are due to the intermodulation products (IMPs) of the input signal and the switch control signal after the signal passes through the switch, so it can be seen that the bandwidth of the filtering delay network module has a critical effect on the system. As shown in Fig. 4, due to the limited bandwidth of the filter, only the fundamental tone and a small portion of the IMPs can be obtained, although most of the signal power is

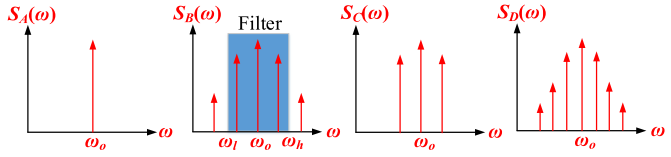

Fig. 4. Spectrum of the signal in the proposed nonmagnetic filtering circulator.

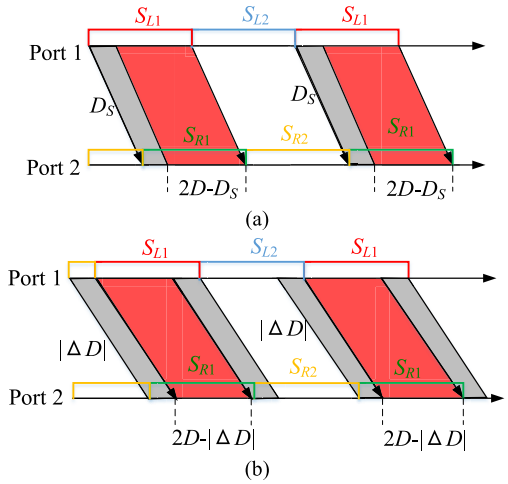

Fig. 5. Impacts of (a) switch rising/falling times and (b) delay time fluctuation on the transmission coefficients.

provided by the fundamental tone and the first-order IMPs, but the broadband performance can minimize the system's IL. The IL can be calculated as follows:

$$IL = -10\log \times \left[\sum 2|a_n|^2 \cdot \left[\begin{array}{l} G_{f_h-f_l}(f_o + nf_m - f_l/2 - f_h/2) \\ + G_{f_h-f_l}(f_o + nf_m + f_l/2 + f_h/2) \end{array}\right]\right] \tag{9}$$

$$f_o = f_l + \frac{f_h - f_l}{2} \tag{10}$$

where $G_{f_h-f_l}$ is the window function, and a_n is the Fourier series constant of the square wave, it can be expressed as follows:

$$a_n = \begin{cases} j/n\pi \cdot \sin(n\pi/2), & n > 0 \\ 1/2, & n = 0 \\ -j/n\pi \cdot \sin(n\pi/2), & n > 0. \end{cases} \tag{11}$$

The passband of the filter is from f_l to f_h. From (9), it is clear that as the bandwidth increases, there will be more IMPs in the passband and the IL of the system will decrease.

D. Filtering Nonmagnetic Circulator Analysis

For investigating the characteristics of the proposed nonmagnetic filtering circulator, a prototype based on the ideal filtering delay networks is implemented and analyzed. The delay function of the circulator is implemented by the filtering delay network with a completely flat group delay response. Based on the ideal network, we will analyze the impact of the rising/falling time of switching and the group delay fluctuation.

In general, the system will suffer from additional IL due to the rising/falling time of switching and the group delay fluctuation of the filtering delay networks, which affect the performance of the system, as analyzed in Section II-C. Therefore, in order to gain an insight into the impacts of the rising/falling time of the switching and group delay fluctuation on the transmission coefficient of the proposed nonmagnetic filtering circulator, the theoretical analysis on the rising/falling time of switching and the fluctuation are thus carried out. For the switches, as shown in Fig. 5(a), assuming that the time required for the rising/falling edge of the switch is D_s, and an additional time delay D_s will be generated when the signal is fed through the switches to the filtering delay networks, which can be expressed as follows:

$$D_1(t) = \sum G_{2D-D_S}(t/2D - D_S/4D - 0.5 - N) \tag{12}$$

$$S_B(t) = S_A(t) \cdot S_{L1}(t) \cdot D_1(t) \tag{13}$$

$$S_D(t) = S_A(t - D) \cdot D_1(t - D) \tag{14}$$

where $D_1(t)$ indicates the signal transmitted to the output port after being affected by the time delay D_s. It can be seen from (13), part of the input signal cannot be transmitted to the output port due to the influence of D_s, which will increase the IL of the system.

Similarly, the group delay fluctuation of the filtering delay network will also affect the transmission characteristics, as shown in Fig. 5(b). Assuming the fluctuation of time delay is ΔD, it can be deduced as follows:

$$D_2(t) = \sum G_{2D-|\Delta D|}(t/2D - |\Delta D|/4D - 0.5 - N) \tag{15}$$

$$S_C(t) = S_A(t) \cdot S_{L1}(t) \cdot D_2(t) \tag{16}$$

$$S_D(t) = S_A(t - D - |\Delta D|) \cdot D_2(t - D - |\Delta D|) \tag{17}$$

where $D_2(t)$ indicates the signal that can be transmitted after being affected by ΔD. The signal enters the filtering delay network and part of the signal is not transmitted to the output port due to the deviation of the time delay, which increases the IL of the system.

The effects of the switch rising/falling time as well as the delay fluctuations on the performances of the circulator are investigated. The numerical analysis on the rising/falling time of switching and fluctuation is thus carried out, as shown in Fig. 6. From Fig. 6(a), it can be observed that the good out-of-band suppressions are maintained as the rising/falling time of switching changes. Moreover, the effect of the varying of the switch rising/falling edge time on the IL of the circulator is presented in Fig. 6(a), and it can be seen that the IL of the circulator is gradually deteriorated from −0.2 to −1 dB as the switch rising edge time increased from 0 to 2 ns. When the control signal is 12.5 ns, the effect of the group delay fluctuation of the filtering delay network on the IL of the circulator is presented in Fig. 6(b). It can be seen that the larger the delay fluctuation, the larger the IL of the circulator. The related theories of the filtering delay network and the design process of the filtering nonmagnetic nonreciprocal circulator are presented in Sections III and IV. It is worth noting that neither the switch rising/falling edge time nor the delay fluctuations affect the filtering characteristics of the circulator.

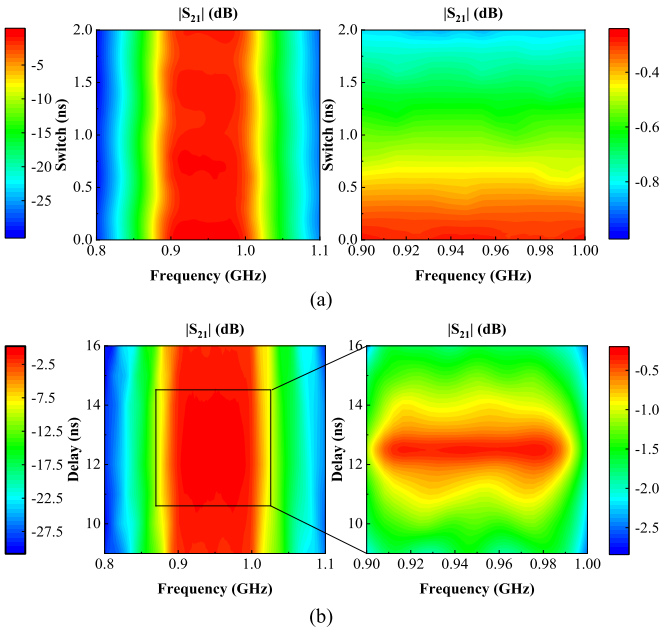

Fig. 6. Impacts of (a) switch rising/falling times and (b) delay time fluctuation on the transmission coefficients.

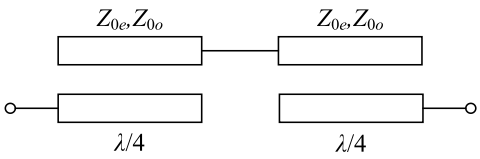

Fig. 7. Coupling units of the filtering network with large flat group delay.

III. Three-Port Circulator Design

Based on the above theoretical analysis, a three-port circulator is designed and proposed, which consists of two independent switching modules and a two microstrip filtering delay networks with large and flat group delay responses. As shown in Fig. 2, the switching module 1 connected with the filtering delay networks is controlled by the signals S_{L1} and S_{L2}, and the switch module 2 is controlled by the signals S_{R1} and S_{R2}, respectively. As two important parts of the proposed filtering nonmagnetic circulator, the characteristics of the filtering delay network and the switch module are investigated in detail as follows.

A. Filtering Delay Network Module

The conventional delay lines are bulky and do not have frequency-selective characteristics. To integrate the filtering and delay characteristics together, a filtering delay network is proposed based on the coupled line structure.

As the basic unit of the proposed filtering delay network, the $\lambda/4$ microstrip coupled network model is shown in Fig. 7, and its odd- and even-mode impedances can be represented in terms of the normalized impedance Z_0, $Z_0 = (Z_e Z_o)^{1/2}$ [28], [29]

$$Z_e = Z_0\sqrt{\frac{1+C_f}{1-C_f}}, \quad Z_o = Z_0\sqrt{\frac{1-C_f}{1+C_f}}, \quad \text{and}$$

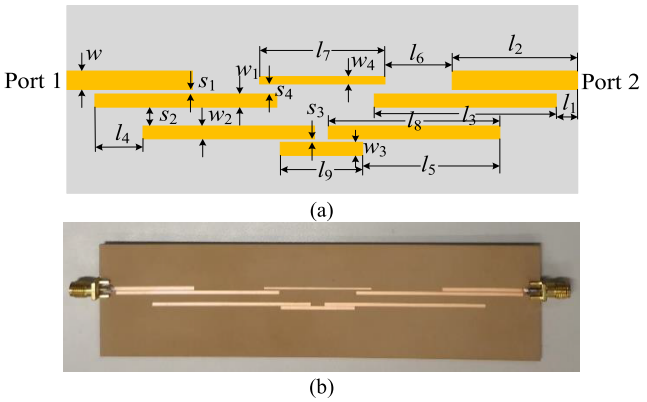

Fig. 8. (a) Structure of the microstrip filtering delay network. (b) Photograph of the microstrip filtering delay network.

$$C_f = \frac{Z_e - Z_o}{Z_e + Z_o} \tag{18}$$

where C_f is the coupling coefficient, and then, the Z-parameter can be expressed as follows:

$$[Z] = \begin{bmatrix} -j\dfrac{Z_0}{\sqrt{1-C_f^2}}\cot\dfrac{\pi f}{2f_0} & -j\dfrac{Z_0 C_f}{\sqrt{1-C_f^2}}\csc\dfrac{\pi f}{2f_0} \\ -j\dfrac{Z_0 C_f}{\sqrt{1-C_f^2}}\csc\dfrac{\pi f}{2f_0} & -j\dfrac{Z_0}{\sqrt{1-C_f^2}}\cot\dfrac{\pi f}{2f_0} \end{bmatrix} \tag{19}$$

where f is the operating frequency, and f_0 is the center frequency, the input impedance can be derived from the Z-parameter as follows:

$$Z_{\text{in}} = Z_{11} - \frac{Z_{12}Z_{21}}{Z_{22}+Z_L}. \tag{20}$$

The group delay and transmission coefficient of this coupled network structure can be expressed as follows:

$$\tau = -\frac{1}{2\pi}\frac{d\angle S_{21}}{df} \tag{21}$$

$$S_{21} = \frac{Z_{\text{ine}} - Z_{\text{ino}}}{(Z_{\text{ine}}+1)(Z_{\text{ino}}+1)} \tag{22}$$

where Z_{ine} is the value of Z_{in} when Z_L is 0 and Z_{ino} is the value of Z_{in} when Z_L is ∞.

From the theoretical analysis of the group delay and transmission coefficient characteristics of the coupled line structure, a filtering delay network with a flat group delay response based on a $\lambda/4$ parallel coupled line is obtained. The proposed microstrip filtering delay network is small in size, simple in structure, as shown in Fig. 8 and has an in-band flat group delay, which can be seen from Fig. 9. The detailed parameters of the filtering delay network are shown in Table I. The impact of l_4 on the group delay response and S-parameters is shown in Fig. 9. It can be seen that as l_4 increases, the group delay response becomes flatter.

The prototype of the proposed filtering delay network is fabricated on Rogers/duroid 6010 substrates with a thickness of 1.27 mm, a relative permittivity of 10.2, and a loss tangent of 0.0023. The simulated and measured results are shown in Fig. 10, and the measured results agree well with the

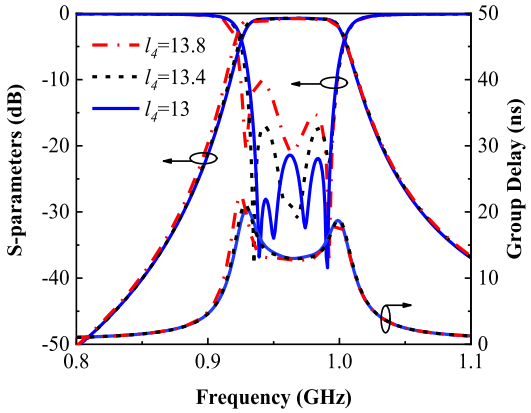

Fig. 9. Impacts of l_4 on the transmission coefficients and group delay of the proposed filtering delay network.

TABLE I
DIMENSIONS OF THE FILTER IN FIG. 10 (UNIT: mm)

w	w_1	w_2	w_3	s_1	s_2	s_3	s_4	h
1.18	1.11	1.11	1.1	0.33	3	0.175	0.1	1.27
l_1	l_2	l_3	l_4	l_5	l_6	l_7	l_8	l_9
6	34	58.4	13	65	25	25	56.6	16

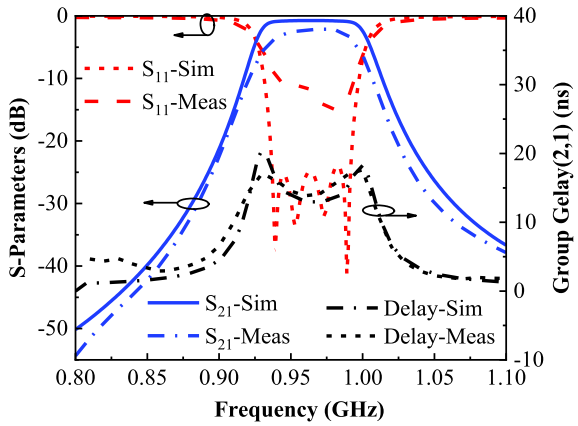

Fig. 10. Simulation and measurement results of the filtering delay network.

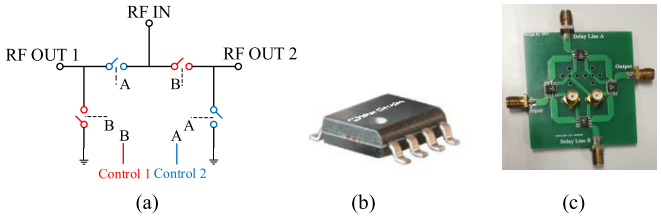

(a) (b) (c)

Fig. 11. (a) Schematic of the MSW 2-20+ [30]. (b) Photograph of the MSW 2-20+. (c) Photograph of the switching module.

simulation ones. It can be seen that good frequency selectivity characteristics are achieved, and the measured/simulated filtering delay network has a flat in-band group delay of 14/14 ns within the frequency band of 925–980 MHz/930–990 MHz, and the IL is better than 1.46/0.89 dB.

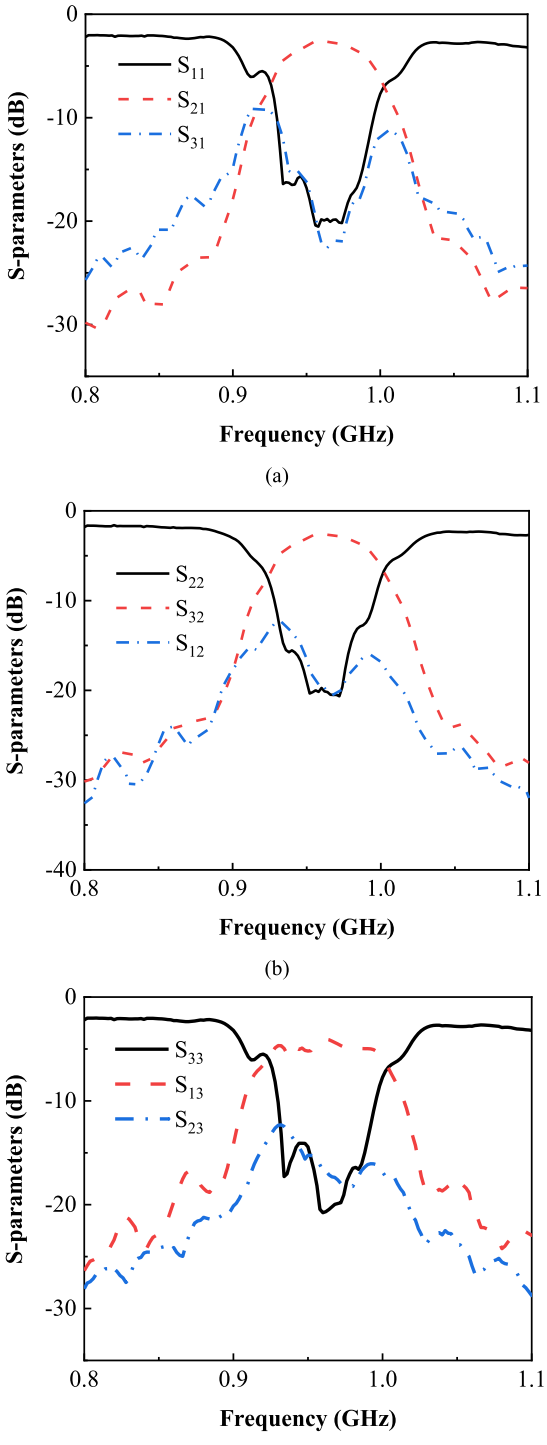

(a) (b) (c)

Fig. 12. Transmission characteristics of the proposed filtering nonmagnetic circulator, when (a) Port 1, (b) Port 2, and (c) Port 3 are excited, respectively.

B. Switch Module

The switch module is composed of four pieces MSW 2-20+, the schematic of the MSW 2-20+ is shown in Fig. 11. Each switch is controlled by two controlling signals (SR/SL) with a phase difference of $2D$. Switch module 1 consists of four MSW 2-20+ with four RF IN ports corresponding to ports 1 and 3 and the filtering delay network modules. The signals from port 1 are multiplexed into the filtering delay network

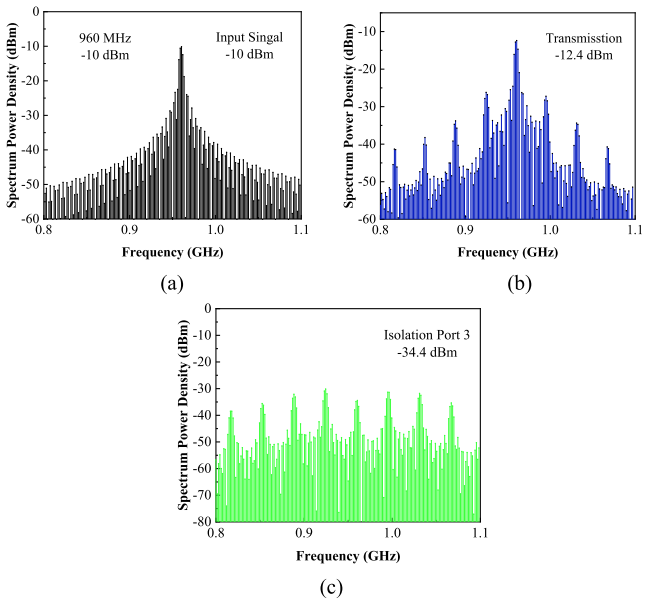

Fig. 13. Simulated spectral content of (a) input signal, (b) transmitted signal at port 2, and (c) transmitted signal at port 3.

module in a time-division sequence by the controlling signal SL. That is, the signals in $0 - 2D$ are fed into the filtering delay network 1 and enter the filtering delay network 2 in $2D - 4D$. The switch module 2 is only composed of a single MSW 2-20+ and is controlled by SR. The signal from port 2 is fed to filtering delay networks 1 and 2 through RF1 and RF2, respectively, which can be seen from Fig. 3.

IV. Simulation and Measurement Result

The circulator is simulated in PathWave Advanced Design System (ADS) [31], the control signal of the switch is simulated by four single pulse signals, and the rising edge time of the switch is set to 2 ns to simulate the opening and closing of the switch. The frequency of the control signal is set to 17.85 MHz ($1/4D$) according to the delay of the filtering delay network is 14 ns. The simulation results are shown in Fig. 12.

It can be seen from Fig. 12 that the filtering circulator operates at 930–990 MHz with an FBW of 6.25%. It can be seen from Fig. 12(a) and (b) that the good filtering characteristics of the circulator are achieved, and the IL is only 2.6 dB when the signal is transmitted from port 1 to port 2 or port 2 to port 3. It can also be seen that good port isolations within the passband of the circulator are achieved, and the isolations are higher than 20 dB. Since the in-band group delay fluctuation of the filtering delay network, IL and port isolations are deteriorated, especially at the edges of the passband.

The spectrum analysis of the simulation is shown in Fig. 13, using a single-tone signal input with a frequency of 960 MHz and a power of −10 dBm. It can be seen that the transmitted signal at port 2 is −12.4 dBm, IL is 2.4 dB, and the highest modulation harmonic tone is 16.2 dBc, caused by the switch and nonflatness of the time delay. The transmitted signal from the isolated port is −34.4 dBm and the highest modulated tone is 24.4 dBc.

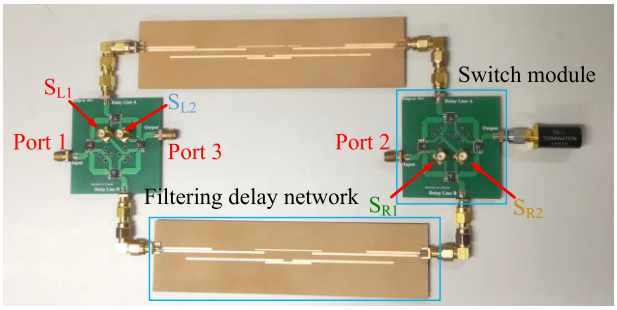

Fig. 14. Photograph of the proposed filtering nonmagnetic circulator.

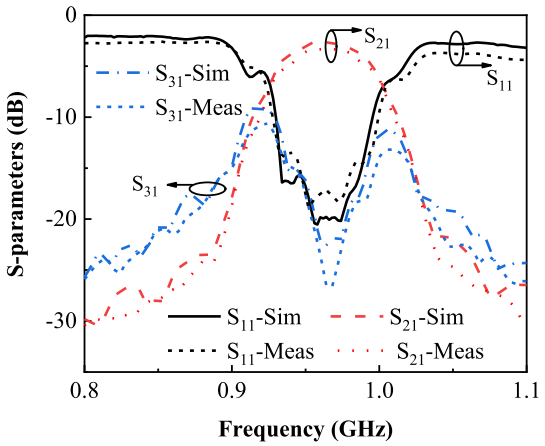

Fig. 15. Measured and simulated results of the filtering nonmagnetic circulator.

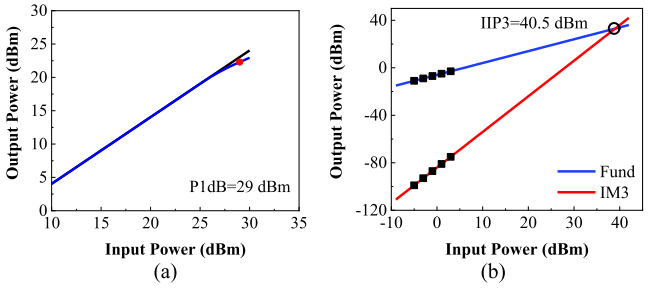

Fig. 16. Measured linearity. (a) P1dB. (b) IIP3.

For demonstration, a prototype of the proposed filtering nonmagnetic circulator is fabricated, assembled, and measured, as shown in Fig. 14. The measurement results of the filtering nonmagnetic circulator are shown in Fig. 15, it can be seen from the results that the measurement results agree with the simulated ones, and the proposed filtering nonmagnetic circulator has good filtering characteristics and loss IL. Moreover, the in-band isolation is greater than 20 dB. Thus, the filtering nonmagnetic circulator with filtering characteristics and high in-band isolation is thus achieved.

The linearity of the circulator was evaluated by measuring the 1-dB input compression point (P1dB) and the input-referred third-order intercept point (IIP3), and Fig. 16(a) shows that the circulator has good linearity with the measured P1dB of 29 dBm because MSW 2-20+ switch has high linearity. (P1dB of the switch is 27 dBm.) The IIP3 measurement was done by transmitting a two-tone signal with frequency spacing

TABLE II
COMPARISON OF OTHER NONMAGNETIC CIRCULATORS

Refs.	CF: f_0 (MHz)	*FBW* (%)	FC*	IX* (dB)	*IL* (dB)	Implementation method
[23]	N/A	N/A	No	30	5	Microstrip
[25]	N/A	N/A	No	32	1	Microstrip
[26]	N/A	N/A	No	40	5	TL
[15]	900	2.6%	Yes	20	2.9	SAW
[20]	1167	0.18%	Yes	15	12	ALN MEMS
[24]	155	5.8%	Yes	20	6.6	MEMS
[27]	146	0.2%	No	15	8	MEMS
This work	**960**	**6.25%**	**Yes**	**22**	**2.6**	**Microstrip**

FC*: the filtering characteristics of the circulator
IX*: the isolation of the circulator

of 2 MHz (959 and 961 MHz), and the measured IIP3 was 40.5 dBm, which is shown in Fig. 16(b).

Table II summarizes the comparison of the proposed work with other nonmagnetic circulators. It can be seen that the proposed filtering nonmagnetic circulator has the advantages of easy integration, lower IL, higher port isolations, and filtering characteristics.

V. CONCLUSION

In this article, a filtering nonmagnetic circulator based on the spatiotemporal modulation of a microstrip filtering delay network using traditional PCB processing technology is proposed. The theory of the proposed filtering nonmagnetic circulator and the filtering delay network with large group delay are analyzed. A three-port circulator is designed and implemented, which has good in-band isolations and filtering performance, and the size of the circulator is reduced due to the integrated design of the nonreciprocal circulator and the filtering delay networks. Moreover, because the processing technology is compatible with the common IC process, the proposed filtering nonmagnetic circulator can be further miniaturized, in addition to integrating the filtering delay work module and the switches module on the same board.

REFERENCES

[1] N. Reiskarimian, A. Nagulu, T. Dinc, and H. Krishnaswamy, "Nonreciprocal electronic devices: A hypothesis turned into reality," *IEEE Microw. Mag.*, vol. 20, no. 4, pp. 94–111, Apr. 2019.

[2] J. Zhou et al., "Integrated full duplex radios," *IEEE Commun. Mag.*, vol. 55, no. 4, pp. 142–151, Apr. 2017.

[3] S. Hong et al., "Applications of self-interference cancellation in 5G and beyond," *IEEE Commun. Mag.*, vol. 52, no. 2, pp. 114–121, Feb. 2014.

[4] D. Bharadia, E. McMilin, and S. Katti, "Full duplex radios," *ACM SIGCOMM Comput. Commun. Rev.*, vol. 43, no. 4, pp. 375–386, Sep. 2013.

[5] D. L. Sounas and A. Alù, "Non-reciprocal photonics based on time modulation," *Nature Photon.*, vol. 11, no. 12, pp. 744–783, Dec. 2017.

[6] A. Goel, B. Analui, and H. Hashemi, "Tunable duplexer with passive feed-forward cancellation to improve the RX-TX isolation," *IEEE Trans. Circuits Syst. I, Reg. Papers*, vol. 62, no. 2, pp. 536–544, Feb. 2015.

[7] A. Kord, D. L. Sounas, and A. Alùs, "Achieving full-duplex communication: Magnetless parametric circulators for full-duplex communication systems," *IEEE Microw. Mag.*, vol. 19, no. 1, pp. 84–90, Jan. 2018.

[8] C. Caloz, A. Alù, S. Tretyakov, D. Sounas, K. Achouri, and Z.-L. Deck-Léger, "Electromagnetic nonreciprocity," *Phys. Rev. Appl.*, vol. 10, no. 4, Oct. 2018, Art. no. 047001.

[9] S. A. Oliver et al., "Integrated self-biased hexaferrite microstrip circulators for millimeter-wavelength applications," *IEEE Trans. Microw. Theory Techn.*, vol. 49, no. 2, pp. 385–387, Feb. 2001.

[10] H. How, X. Zuo, E. Hokanson, L. C. Kempel, and C. Vittoria, "Calculated and measured characteristics of a microstrip line fabricated on a Y-type hexaferrite substrate," *IEEE Trans. Microw. Theory Techn.*, vol. 50, no. 5, pp. 1280–1288, May 2002.

[11] D. L. Sounas, T. Kodera, and C. Caloz, "Electromagnetic modeling of a magnetless nonreciprocal gyrotropic metasurface," *IEEE Trans. Antennas Propag.*, vol. 61, no. 1, pp. 221–231, Jan. 2013.

[12] T. Kodera, D. L. Sounas, and C. Caloz, "Magnetless nonreciprocal metamaterial (MNM) technology: Application to microwave components," *IEEE Trans. Microw. Theory Techn.*, vol. 61, no. 3, pp. 1030–1042, Mar. 2013.

[13] C. Galland, R. Ding, N. C. Harris, T. Baehr-Jones, and M. Hochberg, "Broadband on-chip optical non-reciprocity using phase modulators," *Opt. Exp.*, vol. 21, no. 12, pp. 14500–14511, Jun. 2013.

[14] S. Qin, Q. Xu, and Y. E. Wang, "Nonreciprocal components with distributedly modulated capacitors," *IEEE Trans. Microw. Theory Techn.*, vol. 62, no. 10, pp. 2260–2272, Oct. 2014.

[15] Y. Yu et al., "Radio frequency magnet-free circulators based on spatiotemporal modulation of surface acoustic wave filters," *IEEE Trans. Microw. Theory Techn.*, vol. 67, no. 12, pp. 4773–4782, Dec. 2019.

[16] A. Kord, D. L. Sounas, and A. Alù, "Differential magnetless circulator using modulated bandstop filters," in *IEEE MTT-S Int. Microw. Symp. Dig.*, Jun. 2017, pp. 384–387.

[17] N. A. Estep, D. L. Sounas, and A. Alù, "Magnetless microwave circulators based on spatiotemporally modulated rings of coupled resonators," *IEEE Trans. Microw. Theory Techn.*, vol. 64, no. 2, pp. 502–518, Feb. 2016.

[18] A. Kord, D. L. Sounas, and A. Alù, "Magnet-less circulators based on spatiotemporal modulation of bandstop filters in a delta topology," *IEEE Trans. Microw. Theory Techn.*, vol. 66, no. 2, pp. 911–926, Feb. 2018.

[19] A. Kord, M. Tymchenko, D. L. Sounas, H. Krishnaswamy, and A. Alù, "CMOS integrated magnetless circulators based on spatiotemporal modulation angular-momentum biasing," *IEEE Trans. Microw. Theory Techn.*, vol. 67, no. 7, pp. 2649–2662, Jul. 2019.

[20] C. Xu, E. Calayir, and G. Piazza, "Magnetic-free electrical circulator based on AlN MEMS filters and CMOS RF switches," in *Proc. IEEE Micro Electro Mech. Syst. (MEMS)*, Jan. 2018, pp. 755–758.

[21] C. Xu and G. Piazza, "A generalized model for linear-periodically-time-variant circulators," *Sci. Rep.*, vol. 9, no. 1, p. 8718, Jun. 2019.

[22] G. Chaudhary and Y. Jeong, "Arbitrary prescribed wideband flat group delay circuits using coupled lines," *IEEE Trans. Microw. Theory Techn.*, vol. 66, no. 4, pp. 1885–1894, Apr. 2018.

[23] R. Lu, J. Krol, L. Gao, and S. Gong, "A frequency independent framework for synthesis of programmable non-reciprocal networks," *Sci. Rep.*, vol. 8, no. 1, p. 14655, Oct. 2018.

[24] R. Lu, T. Manzaneque, Y. Yang, L. Gao, A. Gao, and S. Gong, "A radio frequency nonreciprocal network based on switched acoustic delay lines," *IEEE Trans. Microw. Theory Techn.*, vol. 67, no. 4, pp. 1516–1530, Apr. 2019.

[25] J.-A. Wang, D. Li, Y. Liu, Z. Chen, and Z. Zheng, "Novel non-magnetic circulator based on radio frequency nonreciprocal network," in *Proc. Int. Conf. Microw. Millim. Wave Technol. (ICMMT)*, Sep. 2020, pp. 1–4.

[26] M. M. Biedka, R. Zhu, Q. M. Xu, and Y. E. Wang, "Ultra-wide band nonreciprocity through sequentially-switched delay lines," *Sci. Rep.*, vol. 7, no. 1, p. 40014, Jan. 2017.

[27] Y. Yu et al., "Magnetic-free radio frequency circulator based on spatiotemporal commutation of MEMS resonators," in *Proc. IEEE Micro Electro Mech. Syst. (MEMS)*, Jan. 2018, pp. 154–157.

[28] H.-R. Ahn, *Asymmetric Passive Components in Microwave Integrated Circuits*. New York, NY, USA: Wiley, 2006.

[29] G. Chaudhary and Y. Jeong, "Transmission-type negative group delay networks using coupled line doublet structure," *IET Microw., Antennas Propag.*, vol. 9, no. 8, pp. 748–754, Jun. 2015.

[30] *MSW 2-20+, Mini-Circuits*. [Online]. Available: https://www.minicircuits.com/WebStore/dashboard.html?model=MSW-2-20%2B

[31] *ADS-Advanced Design System*, Keysight Technologies, EEsof, Santa Rosa, CA, USA, 2019. [Online]. Available: https://www.keysight.com

Daotong Li (Senior Member, IEEE) received the Ph.D. degree in electromagnetic field and microwave technology from the University of Electronic Science and Technology of China (UESTC), Chengdu, China, in 2016.

In 2017, he joined the Center of Communication and Tracking Telemetry Command, Chongqing University, Chongqing, China, as an Assistant Professor. Since 2015, he has been a Visiting Researcher with the Department of Electrical and Computer Engineering, University of Illinois at Urbana–Champaign, Urbana, IL, USA, with the financial support from the China Scholarship Council. Since 2019, he has been promoted to an Associate Professor. He is currently with the Center of Communication and Tracking Telemetry Command, Chongqing University. He has authored or coauthored more than 100 peer-reviewed journal and conference papers. His current research interests include RF, microwave and millimeter-wave technology and applications, microwave power transmission (MPT), antennas, devices, circuits and systems, and passive and active (sub-) millimeter-wave imaging and radiometer.

Dr. Li has been awarded a Fellowship from the Japan Society for the Promotion of Science (JSPS) and the JSPS Fellow with the Department of Communications Engineering, Graduate School of Engineering, Tohoku University, since November 2021. He was a recipient of the UESTC Outstanding Graduate Awards by the Sichuan Province and UESTC in 2016 and the National Graduate Student Scholarship from the Ministry of Education, China, and "Tang Lixin" Scholarship. He is serving as a reviewer for several IEEE and IET journals, and many international conferences as a TPC Member, a Session Organizer, and the Session Chair.

Chen Yang received the B.S. degree in communication engineering from Chongqing University (CQU), Chongqing, China, in 2021, where he is currently pursuing the M.S. degree in information and communication engineering.

His research interests include nonmagnetic nonreciprocal filters and circulators.

Ying Liu received the B.E. degree in communications engineering from the Qingdao University of Science and Technology, Qingdao, Shandong, China, in 2012, and the M.S. degree in communication and information system from Chongqing University, Chongqing, China, in 2015, where she is currently with the School of Microelectronics and Communication Engineering.

Her current research interests include microwave and optical image processing, and microwave photonics.

Luqi Zhang received the B.S. degree in electronic information science and technology from China West Normal University (CWNU), Nanchong, China, in 2021. She is currently pursuing the M.S. degree in information and communication engineering at Chongqing University (CQU), Chongqing, China.

Her current research interests include planar multifunctional microwave and millimeter-wave passive components.

Qiang Chen (Senior Member, IEEE) received the B.E. degree from Xidian University, Xi'an, China, in 1986, and the M.E. and D.E. degrees from Tohoku University, Sendai, Japan, in 1991 and 1994, respectively.

He is currently the Chair Professor of the Electromagnetic Engineering Laboratory, Department of Communications Engineering, Faculty of Engineering, Tohoku University. His primary research interests include antennas, microwave and millimeter waves, electromagnetic measurement, and computational electromagnetics.

Dr. Chen is a Fellow of Institute of Electronics, Information, and Communication Engineers (IEICE). He received the Best Paper Award and Zenichi Kiyasu Award from the IEICE. He served as the Chair for the IEICE Technical Committee on Photonics-Applied Electromagnetic Measurement from 2012 to 2014, the IEICE Technical Committee on Wireless Power Transfer from 2016 to 2018, the IEEE Antennas and Propagation Society Tokyo Chapter from 2017 to 2018, and the IEICE Technical Committee on Antennas and Propagation from 2019 to 2021.